Output Power Optimization in 980-nm Pumping Lasers Wavelength-Locked Using Fiber Bragg Gratings

by Akira Mugino * *and Yuichiro Irie* *2

ABSTRACT When erbium-doped fiber amplifiers are pumped by 980-nm laser, fluctuations in the pumping wavelength result in large variations in the gain and amplified output in the 1550-nm band --a phenomenon known as pump-mediated inhomogeneity (PMI)--resulting in stricter requirements with respect to wavelength variation in 980-nm laser modules.

Pumping lasers have been developed that use a fiber Bragg grating (FBG) to suppress these pumping wavelength fluctuations, but output power levels using an FBG for wavelength feedback tend to be lower than without an FBG.

This output power drop must be kept as low as possible, and to this end the authors have carried out an analysis involving FBG reflectivity, laser front-facet reflectivity, the wavelength pulling effect and the spatial hole-burning (SHB) effect. This paper discusses the concept of output power optimization for 980-nm laser modules with FBGs, and presents a theoretical analysis and simulation results.

1. INTRODUCTION

One of the advantages of erbium-doped fiber amplifiers (EDFAs) using a 980-nm pumping laser is low noise and low temperature dependence of the gain characteristic. Ordinary 980-nm laser modules, however, experience a wavelength shift proportional to current injection that is generally 0.03 nm/mA to the long-wavelength side. In configuring dense wavelength-division multiplexing (DWDM) systems, on the other hand, it is desirable to use an EDFA with a gain that is made independent of the number of channels that are "on" by controlling the injection current of the pumping laser module to regulate EDFA amplification.

But if injection current changes, the output wavelength of the pumping laser will also change. The change in pumping wavelength will reflect the amplification output characteristics at 1550 nm, and gain fluctuation will soon exceed 1 dB. This phenomenon is known as pump-mediated inhomogeneity, or PMI. [1)]

Considerable effort has been expended to develop pumping lasers using FBGs as a means of suppressing this fluctuation in pumping wavelength, but this has the disadvantage that output power levels of lasers using an FBG for wavelength feedback are always lower than for those without an FBG. Minimizing this power drop requires optimization of FBG reflectivity and laser front-facet reflectivity, and this in turn necessitates analysis that takes account of the wavelength pulling effect and the spatial hole-burning (SHB) effect. This paper presents the results of simulations, and introduces the concept of optimized design of output power characteristics for a 980-nm laser with FBG.

* WA Team, Yokohama R & D Lab., R & D Div.
*2 980-nm Laser Module Team, Yokohama R & D Lab., R & D Div.

2. MODULE STRUCTURE

Figure 1 shows the structure of an actual laser module. The fabrication process involves first bonding the laser chip on the submount, inserting it into the package, centering the chip using a wedge-shaped lensed fiber, and final YAG welding to complete the module. The empirical

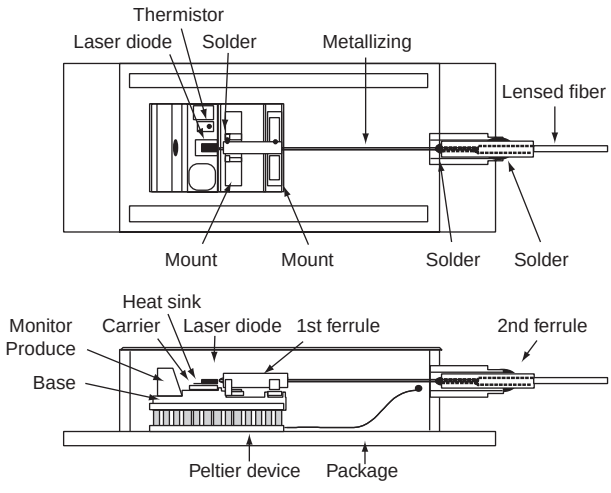

Figure 1 Structure of 980-nm laser module

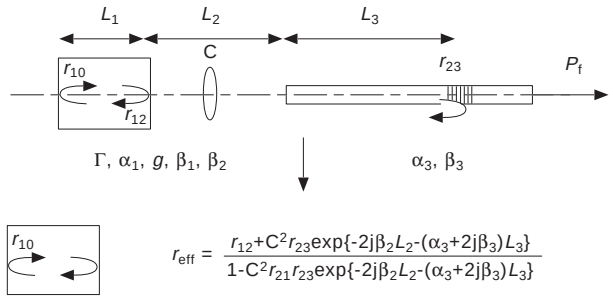

Figure 2 Simplified model for analyzing external cavity resonator using the concept of effective reflectivity R_{eff}

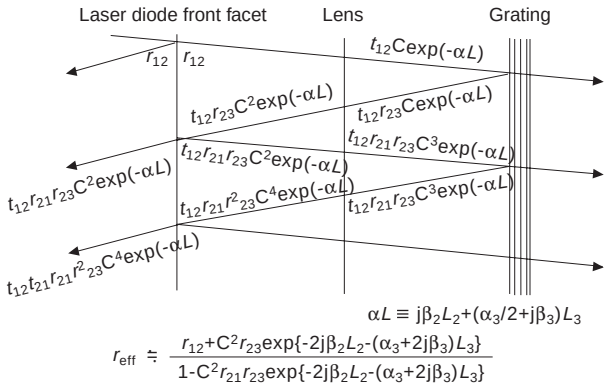

Figure 3 External cavity model for elucidating amplitude reflectivity r_{eff}

average coupling efficiency of laser and fiber was approximately 75-80%, [2] an improvement of about 10% compared to previous symmetrical 2-lens systems. In the structure illustrated in Figure 1, the laser chip is fixed to the package by means of the submount, and the leading end of the wedged fiber and the front facet of the laser chip are separated by several microns. The 1st ferrule is mounted on the pre-stage base by YAG welding, and the 2nd ferrule is attached at the neck by a solder encapsulating process. In this way the module that constitutes the coupling system for the laser and fiber can be modeled to simplify analysis.

3. ANALYTICAL MODEL

Figure 2 is a simplified diagram of a system for coupling the lensed fiber with grating to a laser chip. The following discussion will be conducted in terms of this simplified coupling system.

Simulations of the various characteristics of an FBG external cavity [6] were carried out using coupling efficiency C, FBG reflectivity r_{23}, reflectivity of the front facet of the laser r_{12} (with an anti-reflection (AR) coating), reflectivity of the rear facet of the laser r_{10} (with a high-reflectivity coating), and various laser chip parameters.

There are two points that are the most important for the design of a 980-nm laser module with FBG. They are:

1) the maximum possible output power must be obtained; and
2) since it is necessary, for any given current or temperature, that the lasing wavelength be pulled in from the inherent lasing wavelength to the FBG reflected center wavelength and lase at the FBG wavelength, the range of wavelengths that are pulled should be as wide as possible.

That is to say the module should achieve the optimum trade-off between output power and pulling width. At this point as an analytical tool, we first relate the reflectivity of the anti-reflection coating of the front facet and FBG reflectivity to the effective reflectivity shown in Figure 2 and derive the effective reflectivity. Because of the large number of modes in which lasing can occur, we define reflectivity in the main mode, which has the greatest intensity, as effective reflectivity R_{eff}. Next it is necessary to obtain accurate data on output power, taking into account the SHB phenomenon, which is due to inequality of carrier density within the laser chip caused by the AR and HR reflectivity of the chip. That is to say it is possible to optimize output power by determining the laser module output characteristics corresponding to the effective reflectivity. In Section 4 below, we will find the optimum combination of AR and FBG reflectivity. There will also be a detailed discussion on the optimum trade-off between the settings for output power and the pulling width.

4. EFFECTIVE REFLECTIVITY AND EXTERNAL CAVITY MIRROR LOSS

Effective reflectivity R_{eff} was found by taking absolute values for the combination of reflected and transmitted components at the interfaces of the laser diode front facet, lensed fiber, grating, etc. shown in Figure 3. If, using effective reflectivity R_{eff} (r_{eff} is amplitude and R_{eff} is power reflectivity) in stead of the front-facet and rear-facet reflectivity of an ordinary laser (here r_{10} and r_{eff}), we can obtain a threshold condition equation as shown in Equation (1).

We may then rewrite the mirror loss from this threshold condition equation as Equation (2).

It should be noted that this differs from the so-called mirror loss 1/L x 1n (R) as ordinarily used in that it is multi-element, and it is a dimensionless value not divided by length.

$$r_{10} \times \frac{r_{12}+C^2 r_{23}\exp\{-2j\beta_2 L_2-(\alpha_3+2j\beta_3)L_3\}}{1-C^2 r_{21} r_{23}\exp\{-2j\beta_2 L_2-(\alpha_3+2j\beta_3)L_3\}} \times \exp\{-\Gamma(\alpha_1-g)+2j\beta_1 L_1\}=1 \quad (1)$$

$$\ln\left[\frac{1}{r_{10}} \times \frac{1-C^2 r_{21} r_{23}\exp\{-2j\beta_2 L_2-(\alpha_3+2j\beta_3)(L_3+L_{geff})\}}{r_{12}+C^2 r_{23}\exp\{-2j\beta_2 L_2-(\alpha_3+2j\beta_3)(L_3+L_{geff})\}}\right] \quad (2)$$

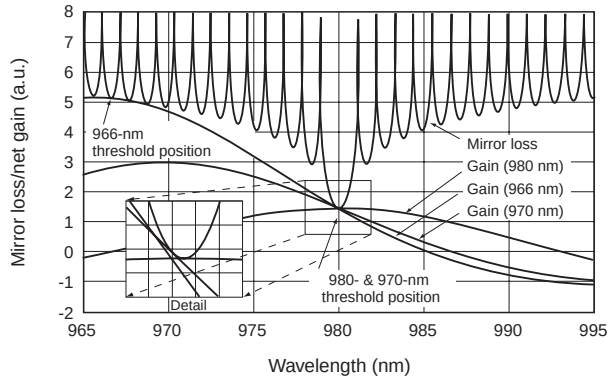

Figure 4 Mirror loss and net gain vs. gain peak wavelength under threshold condition

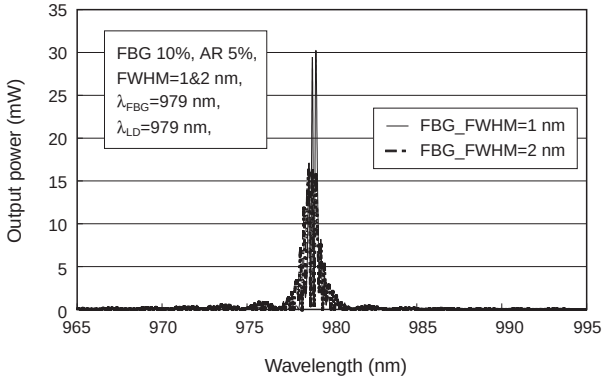

Figure 5 Comparison of spectrum properties using FBGs with FWHM set to 1 nm and 2 nm

5. PULLING WIDTH

In this section we describe the mechanism of wavelength locking by the FBG by introducing the concept of pulling. It is possible to find the various longitudinal modes (spectrum output) at which an external cavity laser can lase by means of numerical analysis of mirror loss and net gain as shown in Equation (2) and derived from the threshold condition in Equation (1).[3), 4)] Figure 4, for example, is a spectrum diagram showing the relationship between mirror loss and net gain for an ideal external cavity (AR=0) for laser gain peak wavelengths λ_{LD} both inside (980 and 970 nm) and outside (966 nm) the pulling range. As can be seen from Figure 4, when a change in laser diode gain is produced by injected current or temperature, the mirror loss characteristics are kept constant by the FBG despite the change in gain peak wavelength, so that the longitudinal lasing mode that satisfies the threshold condition is effectively locked in the vicinity of the FBG reflected center wavelength. It may further be seen that when the value of the gain peak wavelength is separated from the FBG reflected center wavelength by a certain value, normal FBG mode lasing will cease and be replaced by Fabry-Perot-mode lasing in the vicinity of the normal gain peak wavelength (λ_{FP}). This value is hereafter referred to as the pulling width (λ_{pull}). In the example given above, the FBG wavelength λ_{FBG} is set at 980 nm. At AR=0, the theoretical pulling width is approximately 13.9 nm. This may be stated arithmetically as

$$\lambda_{FBG} - \lambda_{FP} = \lambda_{pull} \qquad (3)$$

Thus the pulling width may be defined as shown in Equation (3). It may be pointed out that in fact the pulling width actually differs slightly on the long- and short-wavelength sides of the FBG wavelength, but this distinction will be ignored here.

In designing a pumping laser with FBGs, the first essential is that the lasing wavelength of the diode at the lasing threshold value (or the gain peak wavelength) be within the pulling width on the long-wavelength side of the FBG frequency. It is also indispensable that the total long-wavelength shift of the gain peak wavelength be within the pulling width even if the drive current increases to end-of-life (EOL) under constant temperature conditions. In this case it is best to set the lasing threshold wavelength λ_{lth} shorter than λ_{FBG}, so that, when the difference between the EOL lasing wavelength λ_{EOL} and λ_{lth} is centered on λ_{FBG}, left and right pulling can be achieved.

6. THE EFFECT OF FBG FWHM

Next we investigated the effect of FBG full-width half maximum (FWHM) on pulling width, and it was found that even when the FWHM value fluctuated by 1 or 2 nm, the single-side pulling width varied by only about 0.05 nm, and the increase in lasing threshold current I_{th} was only 0.1 mA. Further investigation of the output spectrum revealed that despite differences in the main lasing mode and spectrum width, the sum of all laser module outputs was the same (see Figure 5). Further, the number of main modes lasing in the FBG was about 7 for a 1-nm FBG and 15 for a 2-nm FBG. Both FBGs have nearly the same free spectral range of almost 0.17 nm, as against a laser diode length of 800 μm. For this reason main mode spacing is virtually determined by diode length.

Investigations into the static properties of the laser--the *L-I* characteristic and lasing wavelength stability--showed that the FWHM value had an extremely large effect. Generally speaking in stable lasing, the *dL*/*dI* value, which is the slope of the output vs. current characteristic, shows a gradual linear decrease to the right. When, on the other hand, repeated unstable lasing occurs with respect to a certain current, the *dL*/*dI* value takes on a kinked form. However the constant change in lasing due to external disturbance is not limited to pumping lasers with FBGs, and main mode lasing may occur on either the short- or long-wavelength side. For this reason if the main lasing mode, which accounts for the greater part of the power, is located in close proximity to the FWHM value of the FBG, and in case it hops to the next longitudinal mode capable of lasing (located outside the FBG FWHM), there will be a marked change in laser output power and kinking of the *L-I* characteristic.

Figure 6 shows the results of experiments on the *L-I* characteristic using FBGs with an FWHM of 1 nm and 2 nm. It can be clearly seen that the *dL*/*dI* characteristic is flatter at the greater FWHM. This may be attributed to the fact that when the FWHM is greater the number of modes within the FWHM increases and the power is averaged.

In addition to stable lasing, however, it may also be desirable to obtain lasing within a narrow range of wavelengths, and if the FWHM of the FBG is too wide, changes in drive current, temperature or the operating environment may broaden the fluctuations in lasing wavelength. Figure 7 shows the gain peak wavelength of a laser chip vs. the lasing wavelength of a laser module. It can be seen that the range of lasing wavelength fluctuation with respect to a change of gain peak wavelength from 970.3 to 987.7 nm is 0.17 and 0.68 nm for FBGs with an FWHM of 1 nm and 2 nm respectively. Taking these results together with the range of wavelength shift due to changes in the environment of the FBG, the fiber temperature coefficient, for example, is approximately 0.01 nm/°C, so that, based on a room temperature of 25°C and an operating temperature range of -20°C to 65°C, there can be a wavelength change of about 0.4 nm. Using an FBG with an FWHM of 0.2 nm, there is a shift of half of 0.68 nm or 0.34 nm (since the pulling width corresponding to the current shift is 8-9 nm), so that there will be an overall wavelength shift of some 0.74 nm. Leaving some leeway, therefore, the permissible range of lasing wavelengths for a pumping laser with FBG is about 1 nm.

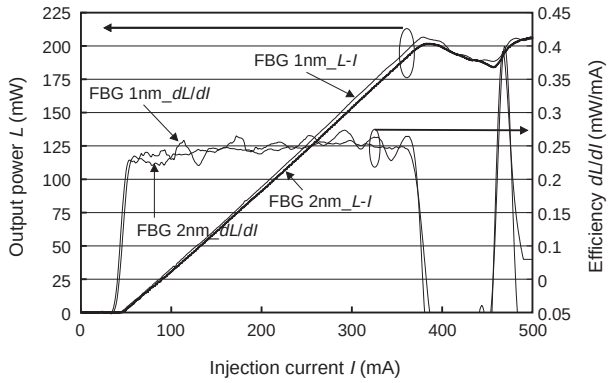

Figure 6 Results of experiments on *L-I* characteristic using FBGs with an FWHM of 1 nm and 2 nm

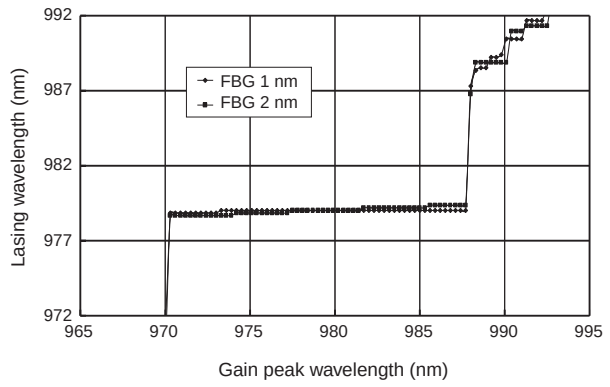

Figure 7 Gain peak wavelength of laser chip vs. lasing wavelength using FBGs with an FWHM of 1 nm and 2 nm

7. AR & FBG REFLECTIVITY AND THE RELATION TO R_{eff}

Next simulations of the interrelationships between effective reflectivity R_{eff} and AR and FBG reflectivity were run, taking account of coupling efficiency *C*. Figure 8 is a 3-dimensional graph derived from the relationships between the various parameters. The equations used are those set forth in Figure 3.

The most striking finding is that there are major differences in R_{eff}, depending on coupling efficiency *C*. For example at AR=1% and FBG=6%, R_{eff} was 6.5%, 7.75% and 9.82% at a *C* of 65%, 75% and 90%, respectively. As a typical case, Figure 8 shows the relationships between R_{eff} and AR and FBG reflectivity where *C* is 75%. We find, for example, that if we take AR reflectivity as constant and seek to establish the change in FBG, the change in R_{eff} will take the form of a rightward-rising curve, whereas if we seek to establish the change in AR with FBG constant, the curve will be rightward-falling as AR becomes larger. It can also be seen that at the same level of R_{eff}, there are a number of combination patterns of AR and FBG reflectivity.

When the AR coating is actually applied to the laser chip, the chip is fabricated with a specific value in view so that it is necessary to know what value of FBG reflectivity should be adopted. In the following section, instead of R_{eff} and AR, as described above, we discus a method of optimizing laser output power using the model shown in Figure 2.

8. OUTPUT POWER CALCULATIONS, TAKING ACCOUNT OF SHB

With pumping lasers for EDFAs, the most important thing is to obtain the highest output power possible. The most commonly used method involves holding down the reflec-

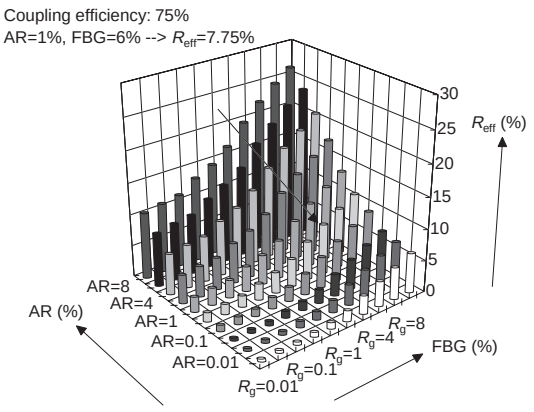

Figure 8 Relationships between AR (1%) and FBG reflectivity and R_{eff} with 75% coupling coefficient

tivity of the laser chip front facet and applying an HR coating to the rear facet, so that higher power is obtained from the front facet. This is because it is characteristic that output power increases monotonously with respect to front facet reflectivity. In actual fact, however, a large optical output signifies a large consumption of the carrier density inside the laser: high power but low carrier density at the front facet, and low output but high carrier density at the rear facet. On the other hand, the carrier (current), which is being injected uniformly from the laser electrode, is producing a process of electron-to-photon conversion over the whole of the axial length of the laser. The carrier density is therefore dependent on facet reflectivity near both facets, and is not uniformly distributed. This gives rise to SHB, creating a phenomenon in which the laser front facet output saturates with respect to reflectivity.[5)~7)]

Thus there is an optimum reflectivity (AR reflectivity) that results in maximum output power. Further, when configuring an external cavity with an FBG, as shown in Figure 2, the front facet reflectivity becomes equivalent to R_{eff}, so that in fact the optimum reflectivity corresponds to R_{eff}.

As was stated in the section above, there are a number of combinations of AR and FBG reflectivity for a given value of R_{eff}, so that if AR is established, optimization can be achieved by appropriate selection of the FBG.

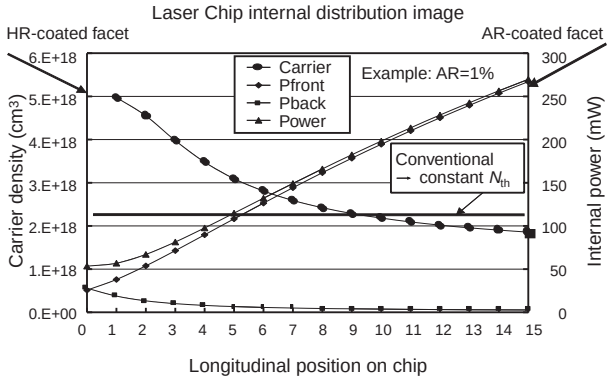

Figure 9 Distribution of carrier density and internal power in the propagation direction of laser chip

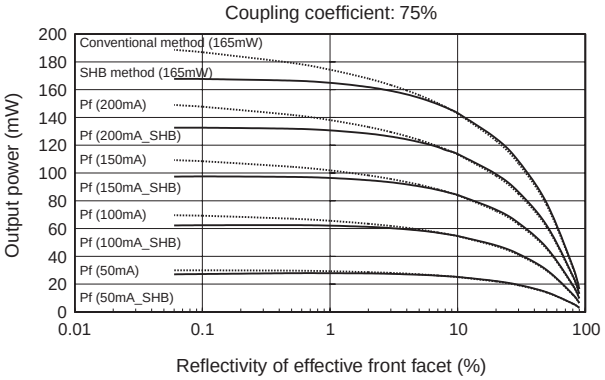

Figure 10 Comparison of analyses of output power of a 980-nm laser diode module using conventional and SHB methods

The graph in Figure 9 models the front and rear output facets on the left and right axes, respectively, and shows the optical power distribution to the front facet and AR coating film and the carrier density distribution. A calculation in which carrier density N_{th} derived from the lasing threshold condition is constant, without taking SHB into account, may be termed the conventional method. It can be clearly seen in Figure 9 that the distribution of carriers consumed by SHB is not uniformly distributed. The data on the graph shown as P_{front} and P_{back} represent the output power of the front and rear facets respectively. Power, then, is the sum of P_{front} and P_{back}. Since this calculation gives not only the optimum value of front facet AR reflectivity but also the facet output strength level, it is also possible to find the breakdown strength from the facet density. Figure 10 shows the relationship between the comparison of analyses of output power and the front facet reflectivity (AR and R_{eff}) for a 980-nm laser diode module at a coupling coefficient of 75% using conventional and SHB methods.

In the conventional calculation, output goes up monotonously as the front facet reflectivity decreases, whereas in calculations taking account of SHB, it is clearly seen that output power saturates at a given front facet reflectivity. It is the front facet reflectivity immediately prior to this saturation that is the optimum value. Thus it is possible to estimate the output power of a laser module with FBG if calculation is done by the SHB method using R_{eff} instead of front facet reflectivity (AR reflectivity). In this way the optimum FBG reflectivity can be determined for any given AR reflectivity, and it is possible to optimize the design by establishing the relationships between the power degradation percentage and the pulling width, in comparison with the case in which there is no FBG. Based on the fact that a greater pulling width can be obtained when AR reflectivity is low, calculations were made with AR=1% and the results are shown in Figure 11.

Figure 11 gives the important design guidelines. The first step in the process of optimization is to establish an AR reflectivity that is just short of output power saturation, and then establishing the FBG reflectivity, taking account of pulling width and power degradation percentage as obtained from a graph such as the one shown in Figure

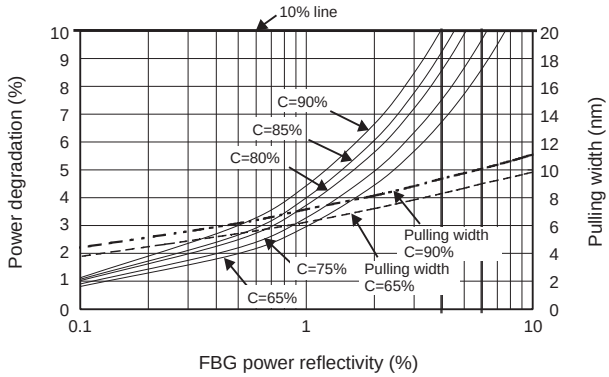

Figure 11 Power degradation percentage and wavelength pulling width relative to FBG power reflectivity, where AR=1%

Table 1 Pulling width at different combinations of AR and FBG reflectivity

AR reflectivity / FBG reflectivity	1%	5%	Difference due to AR
6%	9.5 nm	8.02 nm	1.48 nm
10%	10.5 nm	8.9 nm	1.6 nm
Difference due to FBG	1 nm	0.88 nm	

11. Using the example in Figure 11, the FBG wavelength is 979 nm and the limiting value for gain peak wavelength, assuming a desired pulling width of 8-10 nm, would be 970 nm on the short-wavelength side and 988 nm on the long-wavelength side. If a power degradation percentage of 10% is then set as the limit, and assuming a coupling efficiency by YAG welding of 65-90%, the range of reflectivity in which the FBG can be used will obviously be 4-6%.

9. SUMMARY

There are two ways to increase pulling width: reducing AR reflectivity and increasing FBG reflectivity. Table 1 compares AR and FBG reflectivity for the major laser modules, and shows that in all cases a decrease in AR results in a comparatively wide pulling width. Further, the fact that in Figure 11 the power degradation percentage is larger the higher the coupling efficiency, is due to the fact that R_{eff} is proportional to coupling efficiency as in Figure 3. Since the larger the coupling efficiency the higher the output, it is obviously better to have a higher coupling efficiency.

From the above discussion, pulling width, power output and power degradation percentage are optimized by the optimum selection of AR reflectivity and FBG reflectivity, and the FWHM of the FBG requires comprehensive consideration of *I-L* characteristics, output power stability, kink current, etc. To sum up, the recommended values are an AR of about 1-2% and an FBG FWHM of about 2 nm.

10. CONCLUSION

In optimizing the output power of a pumping laser with FBG, there are many parameters that must be considered. They also affect each other rendering a perfect optimization difficult. In this paper we have set forth aspects of design optimization taking into account an effective reflectivity model and the spatial hole-burning effect with respect to the design concept for producing FBG-mode lasing in a stable, narrow wavelength range (within 1 nm), based on AR reflectivity and FBG reflectivity. Using this design, it is proposed to fabricate a 980-nm pumping laser with FBG having good characteristics.

REFERENCES

1) NE Jolley and F Davis, OAA, TuD6-1, pp.139-142, 1998.
2) Akira Mugino et.al. : IEICE, Autumn National Convention Record, C-3-105, 1997.
3) Akira Mugino et.al. : IEICE, Spring National Convention Record, C-4-16, 1998.
4) Akira Mugino et.al.: Technical report of IEICE,LQE-7,1998.
5) Akira Mugino et.al. : IOOC/OFC'99 , TuC4, pp.29-31,1999.
6) Akira Mugino, (invited) Photonics East '99, Critical Reviews, CR73-09, Boston, 1999.
7) T. Higashi et al, IEEE J.QE Vol.29 No.6, pp.1918-1923, 1993.

Manuscript received on December 1, 1999.